BIO DESIGN

Crystallization and X-ray crystallographic analysis of the PH-like domain of lipid transfer protein anchored at membrane contact sites from *Saccharomyces cerevisiae*

Junsen Tong and Young Jun Im*
College of Pharmacy, Chonnam National University, Gwangju, 61186, Republic of Korea
*Correspondence: imyoungjun@jnu.ac.kr

Lam6 is a member of sterol-specific lipid transfer proteins anchored at membrane contact sites (LAMs). Lam6 localizes to the ER-mitochondria contact sites by its PH-like domain and the C-terminal transmembrane helix. Here, we purified and crystallized the Lam6 PH-like domain from *Saccharomyces cerevisiae*. To aid crystallization of the Lam6 PH-like domain, T4 lysozyme was fused to the N-terminus of the Lam6 PH-like domain with a short dipeptide linker, GlySer. The fusion protein was crystallized under the condition of 0.1 M HEPES-HCl pH 7.0, 10% (w/v) PEG 8000, and 0.1 M Na$_3$Citrate at 293K. X-ray diffraction data of the crystals were collected to 2.4 Å resolution using synchrotron radiation. The crystals belong to the orthorhombic space group P2$_1$2$_1$2$_1$ with unit cell parameters a = 59.5 Å, b = 60.1 Å, and c = 105.6 Å. The asymmetric unit contains one T4L-Lam6 molecule with a solvent content of 58.7%. The initial attempt to solve the structure by molecular replacement using the T4 lysozyme structure was successful.

INTRODUCTION

Intracellular sterol distribution between the endoplasmic reticulum (ER) and other membrane organelles is a fundamental process for the regulation of membrane properties, signal transduction and protein trafficking (Mesmin and Maxfield, 2009; Soffientini and Graham, 2016). Although the ER is the site of cholesterol biosynthesis, it contains only 0.5 – 1% of cellular cholesterol (Maxfield and Wustner, 2002), suggesting transport mechanism exists to transfer the sterol across the cytoplasm between the ER and other membranes. The major route of sterol transport is non-vesicular mechanism mediated by soluble lipid transfer proteins (LTPs), even for organelles linked by transport vesicles (Holthuis and Levine, 2005; Voelker, 2009). LTPs are characterized by the presence of one or more lipid-binding domains, which contain an internal cavity often capped with a flexible lid and allow the extraction of a water-insoluble lipid into the hydrophobic cavity and transfer it through the cytosol (Wong et al., 2017).

Membrane contact sites (MCSs) are close appositions of two membranes within the typical distance of 30 nm, which allows a short distance of transport and close tethering of the proteins involved in these processes (Helle et al., 2013). Lipid transfer proteins anchored at membrane contact sites (LAMs) were discovered recently as new members of the LTP superfamily and were suggested to have sterol transport and regulatory roles at contact sites between the ER and other organellar membranes (Elbaz-Alon et al., 2015; Gatta et al., 2015; Murley et al., 2015). Humans have three LAM homologs, and the budding yeast has six homologs. LAMs are basically integral membrane proteins with a C-terminal transmembrane helix that anchors the proteins to the ER membrane. In addition, LAM homologs commonly contain a PH-like domain that is related to the PH domains found in GRAM (glucosyltransferases, Rab-GTPase activating proteins and myotubularins) family proteins (Wong and Levine, 2016).

Lam6, also named as Ltc1 (lipid transfer at contact site 1), is a relatively short LAM homolog with 693 amino acids and contains a single sterol-transfer domain. Lam6 resides in several contact sites: ERMES (ER/mitochondria encounter structure), vCLAMP (vacuole and mitochondria patch), and NVJ (nuclear vacuolar junction) (Elbaz-Alon et al., 2015; Murley et al., 2015). Lam6 localizes to the ER-mitochondria contacts by its PH-like domain in a Tom70/71-dependent manner. However, the molecular basis of the PH-like domain-mediated targeting is not well understood. PH domains with 100–120 amino acids have a common structural fold consisting of seven-stranded two β-sheets and a C-terminal amphipathic helix. Many PH domains are involved in protein-targeting by their abilities to bind phosphoinositides, and various proteins (Tong et al., 2016).

The LAM PH-like domains are characterized by the presence of an additional N-terminal helix preceding the canonical PH domain topology (Wong and Levine, 2016). However, the LAM PH-like domains display poor sequence homologies to the typical PH domains and have no sequence similarity to the proteins of known structures in the Protein Data Bank.

In this study, to elucidate the structural features of the Lam6 PH-like domain, we performed crystallization and preliminary x-ray analysis of the Lam6 PH-like domain. To improve protein stability and crystallization properties, we constructed a T4 lysozyme fusion to the Lam6 PH-like domain. We were able to purify and crystallize the fusion protein and obtained X-ray diffraction data at 2.4 Å resolution. Phasing by molecular replacement using a structure of T4 lysozyme was successful, and structure determination is underway.

RESULTS AND DISCUSSION

Initially, we attempted to purify the intact Lam6 PH-like domain (residue 161-272) using a cleavable N-terminal His-tag fusion. The Lam6 PH-like domain displayed low solubility in protein expression and the purified protein was prone to precipitation upon storage at 4℃. We could not obtain crystals of the intact Lam6 PH-like domain. To improve the protein stability and the crystallization properties, we applied an N-terminal T4 lysozyme (T4L) fusion techniques, which have been successfully exploited in the crystallization of various globular proteins including G-protein coupled receptors (Zou et al., 2012). To have a T4L fusion protein suitable for crystallization, the link between T4L and the Lam6 PH-like domain must be short and relatively rigid, yet not interfere with the target protein folding. Therefore, the linker residues between the T4L and Lam6 PH-like domain was limited to two amino-acid residues (GlySer), which originate from the recognition sequence of the BamHI restriction enzyme (Table 1). In addition, the T4L fusion was expected to be advantageous in determining phase information by molecular replacement.

The T4L-Lam6 PH fusion protein was expressed in *E. coli* BL21(DE3) and purified to homogeneity by Ni-NTA and size exclusion chromatography (SEC) (Figure 1A, B). The SEC profile confirmed the fusion protein is a monomer in solution. Proteins were concentrated to 10 mg/ml for crystallization screening.
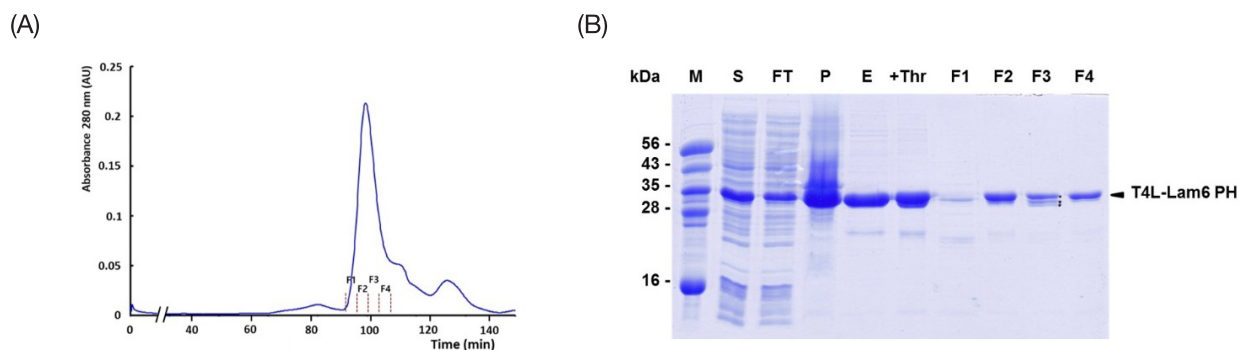
(A)

(B)

FIGURE 1 | **Purification of the T4L-Lam6 PH-like domain.** (A) Elution profile of size exclusion chromatography of the T4L-Lam6 PH fusion protein. (B) SDS-PAGE analysis of the fractions from size-exclusion chromatography. Lane M indicates molecular weight markers; Lane S indicates supernatant after cell lysis; Lane FT indicates flow through in the Ni-NTA affinity chromatography; Lane P indicates pellet after cell lysis; Lane E indicates eluted sample from the Ni-NTA column; Lane Thr indicates the thrombin treated sample of the Ni-NTA eluate; Lanes F1 to F4 indicate SEC fractions in figure 1A.
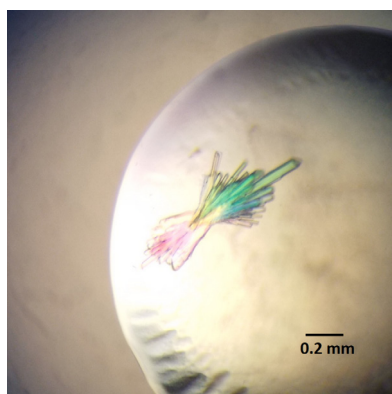

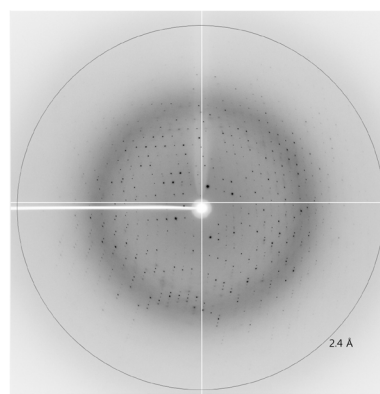FIGURE 2 | Crystal image of the T4L-Lam6 PH-like domain.

FIGURE 3 | Representative diffraction image of the T4L-Lam6 PH-like domain crystal The resolution limit of the data is indicated with a circle.

Needle shape crystals of the T4L-Lam6 PH appeared under the condition of 0.1 M HEPES-HCl pH 7.0, 10% (w/v) PEG 8000, and 0.1 M Na₃Citrate at 293K in seven days with a typical size of 0.02 × 0.02 × 0.2 mm (Table 2, Figure 2). X-ray diffraction data of native crystals were collected at 2.4 Å resolution with 99.0% completeness using the 7A beamline at Pohang Light Source. Crystals belong to the orthorhombic space group $P2_12_12_1$ with unit cell parameters of a = 59.5 Å, b = 60.1 Å, c = 105.6 Å and $α = β = γ = 90°$. The asymmetric unit contains one T4L-Lam6 molecule with a corresponding V_M of 2.98 $Å^3$ Da^{-1} (Table 3).

The phase information for structure determination was calculated by molecular replacement (MR) using the T4L structure as a search model. The molecular weight (m.w.) of T4L is 18,258 Da, which is only 57.6% of the total mass of the T4L-Lam6 PH fusion protein (m.w. 31,683 Da). Therefore, the initial MR phasing based on the T4L structure alone did not produce interpretable maps to assign the individual residues on the Lam6

PH-like domain. Still, the molecular boundaries of the Lam6 PH-like domain could be defined (Figure 4A). The structure of the Osh3 PH domain (Tong et al., 2013) (PDB id: 4IAP) as a starting model was manually located into the electron densities of the Lam6 PH-like domain. The $2F_o$-F_c model maps (Figure 4B) generated with the structures of the T4L and Osh3 PH were further improved by density modification using Resolve and the resulting electron-density maps were readily interpretable. The backbones of the Lam6 PH like domain were well visible in the electron-density maps (Figure 4C). Model building and structure refinements are currently underway.

The forthcoming structure of the T4L-Lam6 PH like domain will provide structural basis of the targeting function of the LAM PH-like domains. This study suggests that the T4L fusion to small target proteins with a short connecting linker could serve as alternative strategies for the design of crystallization constructs, when traditional approaches have failed to yield good crystals.
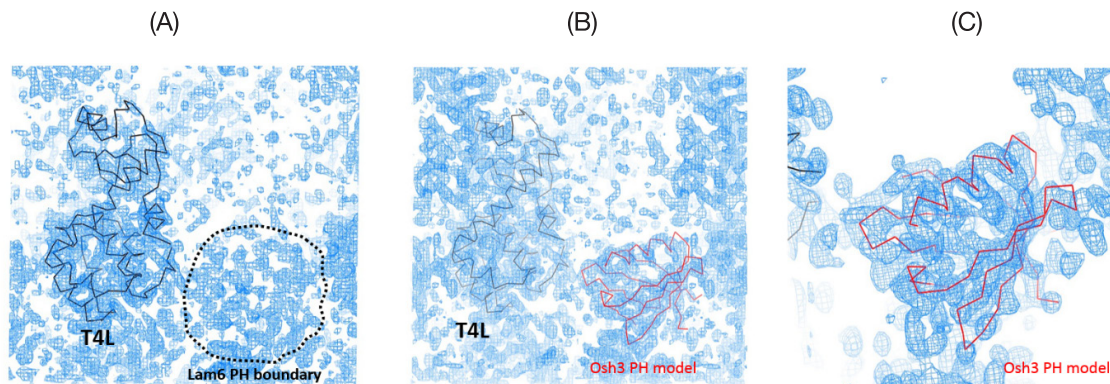
(A)　　　　　　　　　(B)　　　　　　　　　(C)

FIGURE 4 ⏐ Electron density maps generated by MR phasing. (A) Initial $2F_o$-F_c model map (contoured at 1.5$σ$) using a T4L structure as a starting model. (B)The $2F_o$-F_c map (contoured at 1.5$σ$) calculated using the model phases of the T4L and Osh3 PH structures. (C) Density modified map (contoured at 1.0$σ$) calculated by the software Resolve using the $2F_o$-F_c map (B).

TABLE 1 ⏐ Lam6 PH-like domain production information

Source organism	*Saccharomyces cerevisiae* S288C
DNA source	Genomic DNA
UniProt ID	Q08001 (Gene name: Lam6/Ltc1)
Forward primer	GTATAT GGATCC GAGGCTAATAAAAAATTCCG
Reverse primer	GATACA CTCGAG TCA ATTGGTTAAGTTTTCCTTTG
Cloning vector	pHis-Thr-T4L
Expression host	*E. coli* BL21(DE3)
Complete amino acid sequence of the construct produced*	*M*SYYHHHHHHDYDIPT LVPR/GS (NIFEMLRIDEGLRLKIYKNTEGYYTIGIGHLLTKSPSLNAAKSELDKAIGRNTNGVITKDEAEKLFNQDVDAAV RGILRNAKLKPVYDSLDAVRRAALINMVFQMGETGVAGFTNSLRMLQQKRWDEAAVNLAKSRWYNQTPN RAKRVITTFRTGTWDAY) GS **EANKKFRQMFKPLAPNTRLITDYFCYFHREFPYQGRIYLSNTHLCFNSTVLNWMAKLQIPLNEIKYLDK VTTNSSAISVETVTNRYTFSGFIARDEVFQLITRVWSKENLTN**

* The initiating methionine residue is indicated by a bold italic character; the slash (/) indicates the thrombin protease cleavage site; the residues in the parenthesis are the sequence of T4L (residue 2 -161); GS indicates a dipeptide linker; the bold characters indicate the Lam6 PH-like domain sequence.

TABLE 2 | Crystallization

Method	Hanging drop vapor diffusion
Plate type	15-well plate, Qiagen
Temperature (K)	295
Protein concentration (mg ml^{-1})	10
Buffer composition of protein solution	20 mM Tris-HCl pH 7.5, 150 mM NaCl.
Composition of reservoir solution	0.1 M HEPES-HCl pH 7.0, 10% (w/v) PEG 8000, and 0.1 M Na3Citrate.
Volume and ratio of drop	1.2 µl, 1:1
Volume of reservoir (µl)	1000

TABLE 3 | Data collection and processing statistic

X-ray source	PLS-7A
Wavelength (Å)	0.97934
Temperature (K)	100
Detector	ADSC Quantum 270
Crystal-to-detector distance (mm)	260
Rotation range per image (°)	1 (240 images)
Exposure time per image (s)	1
Space group	$P2_12_12_1$
a, b, c (Å)	59.5, 60.1, 105.6
α, β, γ (°)	90, 90, 90
Resolution range (Å)	50 - 2.4 (2.44 – 2.40)
Total number of reflections	123116
Number of unique reflections	15204 (727)
Completeness (%)	99.0 (100.0)
I / σ(I)	48.3 (9.7)
R_{merge} (%)	9.8 (41.2)
Redundancy	8.1 (9.4)
Number of molecules in asymmetric unit	1
V_M (Å^3/Da)	2.98
Solvent contents (%)	58.7

METHODS

Cloning

DNA for the PH-like domain (residues 161-272) of yeast Lam6 (UniProt ID: Q08001) was amplified from *S. cerevisiae* genomic DNA using PCR. The amplified gene was subcloned into the BamHI/Xhol site of a modified pHIS-T4L vector providing an N-terminal T4 lysozyme fusion. The T4L contained four mutations (R12G, C54T, C97A, and I137R), which were introduced to increase the crystallizability of T4L (Rosenbaum et al., 2007). The T4L used in this study contained an additional mutation in the active site residues, D20N, which prevents bacterial cell lysis during protein expression. The T4L has a cleavable N-terminal hexa-histidine tag by thrombin protease. The Lam6 PH-like domain was fused to the C-terminus of a T4 lysozyme (residues 2-160) with GlySer, as a dipeptide linker (Table 1).

Protein purification and crystallization of the T4L-Lam6 PH-like domain

E. coli BL21(DE3) cells were transformed with the plasmid encoding the T4L-Lam6 PH. The recombinant protein was expressed by induction with 0.25 mM isopropyl β- D-1-thiogalactopyranoside (IPTG), when the cell density reached an OD_{600} value of ~0.6. Cells were further incubated for 12 hours at 20℃ and harvested by centrifugation at 3,000 rpm for 20 min. The cells were re-suspended in 2X phosphate buffered saline (PBS) containing 30 mM imidazole and were lysed by sonication. After centrifugation at 13,000 rpm for 45 min, the supernatant containing the His-tagged T4L-Lam6 PH was applied to a Ni-NTA affinity column. The protein was eluted from the column using 0.1 M Tris–HCl pH 6.0, 0.3 M NaCl, 0.3 M imidazole. The protein was concentrated to 10 mg/ml and the N-terminal his-tag was removed by addition of thrombin protease. The T4L-Lam6 PH was subjected to size exclusion chromatography on a Superdex 200 column (GE healthcare) equilibrated with 20 mM Tris-HCl pH 7.5, 150 mM NaCl. The peak fractions containing the T4L-Lam6 PH were concentrated to 10 mg/ml for crystallization.

Initial crystallization screening was carried out using hanging-drop vapor diffusion method, by mixing equal volumes (0.8 µl) of protein solution and customized crystallization solution in 96 well screening plates at 295K. Crystals of the T4L-Lam6 PH appeared in 0.1 M HEPES-HCl pH 7.0, 10% (w/v) PEG 8000, and 0.1 M Na$_3$Citrate after seven days with a maximum size of 0.02 x 0.02 x 0.2 mm.

X-ray data collection and molecular replacement phasing

The crystals were cryoprotected in a reservoir solution supplemented with 30% glycerol and were flash-cooled by immersion in liquid nitrogen. Diffraction data were collected at a fixed wavelength of 0.97934 Å using an ADSC Q270 CCD detector on the 7A beamline at Pohang Light Source (PLS), Pohang Accelerator Laboratory. All data were processed and scaled using HKL-2000. The statistics for the X-ray diffraction data are shown in Table 3. The structure of the Lam6 PH-like domain was solved by molecular replacement using the T4L structure taken from the crystal structure of the Osh3 PH-T4L fusion (PDB id: 4IAP). The Matthews coefficient (V_m) analysis suggested the presence of a single T4L-Lam6 PH molecule in the asymmetric unit with a solvent content of 58.7%. The rotational and translational search using the software PHASER (McCoy et al., 2007) located a single T4L molecule in the asymmetric unit. The initial model maps were not interpretable for residue assignments but showed the molecular boundaries of the PH-like domain. The extended loops of the Osh3 PH (PDB id: 4IAP) were truncated and the core structure of the PH domain was manually located inside the molecular boundaries of the Lam6 PH-like domain. Subsequently, the model maps generated by including Osh3 PH model were further improved by density modification and the resulting density maps were readily interpretable. The model building was done using the software COOT (Emsley et al., 2010).

CONFLICT OF INTEREST
The authors declare that there is no conflict of interest.

ACKNOWLEDGEMENTS

REFERENCES

Elbaz-Alon, Y., Eisenberg-Bord, M., Shinder, V., Stiller, S.B., Shimoni, E., Wiedemann, N., Geiger, T., and Schuldiner, M. (2015). Lam6 Regulates the Extent of Contacts between Organelles. *Cell Rep* **12**, 7-14.

Emsley, P., Lohkamp, B., Scott, W.G., and Cowtan, K. (2010). Features and development of Coot. *Acta Crystallogr D Biol Crystallogr* **66**, 486-501.

Gatta, A.T., Wong, L.H., Sere, Y.Y., Calderon-Norena, D.M., Cockcroft, S., Menon, A.K., and Levine, T.P. (2015). A new family of StART domain proteins at membrane contact sites has a role in ER-PM sterol transport. *Elife* **4**.

Helle, S.C., Kanfer, G., Kolar, K., Lang, A., Michel, A.H., and Kornmann, B. (2013). Organization and function of membrane contact sites. *Biochim Biophys Acta* **1833**, 2526-2541.

Holthuis, J.C., and Levine, T.P. (2005). Lipid traffic: floppy drives and a superhighway. *Nat Rev Mol Cell Biol* **6**, 209-220.

Maxfield, F.R., and Wustner, D. (2002). Intracellular cholesterol transport. *J Clin Invest* **110**, 891-898.

McCoy, A.J., Grosse-Kunstleve, R.W., Adams, P.D., Winn, M.D., Storoni, L.C., and Read, R.J. (2007). Phaser crystallographic software. *J Appl Crystallogr* **40**, 658-674.

Mesmin, B., and Maxfield, F.R. (2009). Intracellular sterol dynamics. *Biochim Biophys Acta* **1791**, 636-645.

Murley, A., Sarsam, R.D., Toulmay, A., Yamada, J., Prinz, W.A., and Nunnari, J. (2015). Ltc1 is an ER-localized sterol transporter and a component of ER-mitochondria and ER-vacuole contacts. *J Cell Biol* **209**, 539-548.

Rosenbaum, D.M., Cherezov, V., Hanson, M.A., Rasmussen, S.G., Thian, F.S., Kobilka, T.S., Choi, H.J., Yao, X.J., Weis, W.I., Stevens, R.C., and Kobilka, B.K. (2007). GPCR engineering yields high-resolution structural insights into beta2-adrenergic receptor function. *Science* **318**, 1266-1273.

Soffientini, U., and Graham, A. (2016). Intracellular cholesterol transport proteins: roles in health and disease. *Clin Sci (Lond)* **130**, 1843-1859.

Tong, J., Manik, M.K., Yang, H., and Im, Y.J. (2016). Structural insights into nonvesicular lipid transport by the oxysterol binding protein homologue family. *Biochim Biophys Acta* **1861**, 928-939.

Tong, J., Yang, H., Yang, H., Eom, S.H., and Im, Y.J. (2013). Structure of Osh3 reveals a conserved mode of phosphoinositide binding in oxysterol-binding proteins. *Structure* **21**, 1203-1213.

Voelker, D.R. (2009). Genetic and biochemical analysis of non-vesicular lipid traffic. *Annu Rev Biochem* **78**, 827-856.

Wong, L.H., Copic, A., and Levine, T.P. (2017). Advances on the Transfer of Lipids by Lipid Transfer Proteins. *Trends Biochem Sci* **42**, 516-530.

Wong, L.H., and Levine, T.P. (2016). Lipid transfer proteins do their thing anchored at membrane contact sites... but what is their thing? *Biochem Soc Trans* **44**, 517-527.

Zou, Y., Weis, W.I., and Kobilka, B.K. (2012). N-terminal T4 lysozyme fusion facilitates crystallization of a G protein coupled receptor. *PLoS One* **7**, e46039.